

RE-215J

PION PRODUCTION IN HIGH ENERGY  
COSMIC RAY COLLISIONS

June 1965

FACILITY FORM 602

(ACCESSION NUMBER)	N 66-12247
(PAGES)	43
(NASA CR OR TMX OR AD NUMBER)	CR-6592
(THRU)	1
(CODE)	29
(CATEGORY)	

*Grunman*

RESEARCH DEPARTMENT

GPO PRICE \$ \_\_\_\_\_  
CFSTI PRICE(S) \$ \_\_\_\_\_  
Hard copy (HC) \_\_\_\_\_  
Microfiche (MF) \_\_\_\_\_

# 653 July 65

PION PRODUCTION IN HIGH ENERGY COSMIC  
RAY COLLISIONS<sup>†</sup>

by

Martin S. Spergel

M. Lieber<sup>‡</sup>

S. N. Milford

Geo-Astrophysics Section

<sup>†</sup> Supported by the National Aeronautics and Space Administration  
under Contract NASw-699.

<sup>‡</sup> Current address: Department of Physics, Harvard University,  
Cambridge, Mass.

Approved by: *Charles E. Mack, Jr.*  
Charles E. Mack, Jr.  
Director of Research

## Summary

The Landau-Milekhin hydrodynamic model of very high energy nucleon interactions is extended to calculate the pion energy and angle distributions in the center of mass system (CMS) and laboratory frames. Consideration of the physical limitations on the average energy of the pions produced in the decomposition of the nucleonic fluids leads to truncation of the pion distribution and a rather slow energy dependence of the average CMS pion energy on the incident proton energy. When a power law dependence is chosen for incident primary cosmic ray protons, the pion production spectrum found in the laboratory frame has a steeper energy spectrum than those found using simpler models of nucleon interactions.

## TABLE OF CONTENTS

<u>Item</u>	<u>Page</u>
1. Introduction .....	1
2. The Landau Model .....	2
3. Pion Energy and Angular Distribution in CMS .....	5
4. Distribution of Pions in Laboratory Frame .....	19
5. The Cosmic Ray Pion Source Function .....	26
References .....	33
Appendix .....	35

## LIST OF TABLES

<u>Table</u>		<u>Page</u>
1	Integral Energy Distribution: $G(E_{\pi}^c)$ .....	18
2	Integral Angular Distribution: $G(\theta^c)$ .....	19
3	Energy Distribution Calculations .....	27
4	Angular Distribution Calculation .....	28

## FIGURE CAPTIONS

Fig. 1. - Nucleon-Nucleon Scattering According to the Landau Model (Adaption of a Figure from AMAI et al.<sup>(5)</sup> ).

Fig. 2. - Pion Transverse Momentum Distribution, after MILEKHIN<sup>(16)</sup>.

Fig. 3. -  $f(\theta^c)$ , the Center of Momentum Angular Distribution of Pions, Given by Eq. (10) in Terms of the Center of Momentum Angle  $\theta^c$ .

Fig. 4. -  $f(E_\pi^c)$ , Center of Mass Energy Distribution of Pions, Given by Eq. (16).

Fig. 5. - Laboratory Energy Distribution of Pions,  $f(E_\pi)$  from Eq. (30).

Fig. 6. - Laboratory Angular Distribution of Pions,  $f(\theta)$  Produced in a Single Collision.

Fig. 7. - Pion Source Function in Space ( $n \sigma_{pp} \equiv 1$ ) from Cosmic Ray Collisions (a) Hydrodynamic Model (Present Paper) (b) GINZBURG - SYROVATSKI<sup>(15)</sup>.

## 1. Introduction

Recent experiments<sup>(1,2)</sup> studying cosmic ray proton collisions at very high energies ( $> 10^{10}$  eV) indicate that a peripheral model of nucleon-nucleon interaction does not explain properly multiple production of mesons at these energies. In this paper therefore, a detailed study is made of a highly inelastic model of nucleon-nucleon collisions. Both the FERMI<sup>(3)</sup> and the LANDAU<sup>(4)</sup> models of nucleon-nucleon collisions are examples of such highly inelastic processes.

The Fermi model characterizes the collision volume of the two nucleons as a highly excited fluid. The fluid is typified by a temperature that is determined by the total center of mass system energy. The fluid decays isotropically into particles with a probability dependent only on the statistical weight of their final states. The total number of particles is proportional to the fourth root of the incident laboratory energy of the cosmic ray proton. The Fermi model has been extensively treated by many authors<sup>(3)</sup>. It has several shortcomings, in particular it predicts many more K mesons and nucleons than are produced, and much higher energies than observed.

The Landau-Milekhin model, like the Fermi model, is hydrodynamical. The colliding nucleons are characterized as colliding fluids. When the nucleons collide they form a highly excited fluid volume that expands according to the laws of relativistic

hydrodynamics. In the early stage of expansion a few high energy pions are ejected. In later stages the fluid cools and finally decomposes into individual mesons. There is some field theoretic justification<sup>(5)</sup> for this model. This model's predictions seem to be reasonably substantiated by the recent data<sup>(1,2)</sup>.

The Landau model, though more complex than the Fermi model, seems fruitful to adopt for further study. It is discussed further in the next section. Section 3 contains the application of the Landau-Milekhin model of pion production to the center of mass system. The laboratory frame is discussed in Section 4; energy distribution functions are introduced which are angle independent. The final section contains an example of the techniques developed in Section 4, in the calculation of the energy spectrum of pions produced by cosmic rays, and some concluding remarks.

## 2. The Landau model

We begin an analysis of the Landau-Milekhin model by establishing notation. Let  $E_p$  be the total energy of the incoming cosmic ray proton, and let the target proton be at rest in the laboratory frame of reference and, if  $c$  is taken as "1", have a rest energy  $M$  ( $\approx 1$  GeV). We define the quantities  $\gamma_p = E_p/M$  and  $\gamma_\pi = E_\pi/\mu$  where  $\mu$  is the pion mass and  $E_\pi$  is the pion total energy. CMS quantities are distinguished by the use of a "c" superscript, while laboratory quantities are not labeled.



The dimensionless energy,  $\gamma$ , is related to the dimensionless velocity,  $\beta$ , by  $\gamma = (1 - \beta^2)^{-\frac{1}{2}}$ . The CMS frame is assumed to move with velocity  $W$  in the laboratory, in the direction of the incident nucleon. We define  $\Gamma = (1 - W^2)^{-\frac{1}{2}}$ , which by elementary kinematics  $\approx [\gamma_p/2]^{\frac{1}{2}}$ . The colliding protons in the CMS will have energy  $E_p^c = M\Gamma$ . We shall always consider  $\gamma_p > 50$ .

According to many experiments, the high energy cross section of a nucleon is approximately its geometrical cross section, with the pion Compton wavelength for a diameter  $\sigma \approx \pi(\hbar/2\mu)^2$ . We assume that a nucleon at rest is a uniform fluid sphere of this cross section. Therefore, in a system where the nucleons are moving with velocity  $W$ , their spheres contract to disks of transverse radius  $\hbar/2\mu$  and thickness  $\hbar/2\mu\Gamma = \Delta$ . The time of collision is of order  $\Delta$  and if a fraction,  $q$ , of the total energy  $2E_p^c$  is transferred to the mesons ( $q$  is frequently called the inelasticity), the "mechanical action" changes by  $\delta s \approx 2qE_p^c \cdot \Delta = \hbar[M/\mu]q$ . Because  $M/\mu \approx 7$ , it follows that  $\delta s \approx 7q\hbar$ . For a classical theory to be valid,  $\delta s \gg \hbar$ , so we must have  $q \sim 1$ . Thus, the Landau theory is limited to highly inelastic collisions.

The Landau model (see Fig. 1) considers that at the instant of contact of the colliding nucleons ( $t = 0$ ), two shock waves begin to propagate into the disks with velocity  $C_0^2$  given by relativistic Rankine-Hugoniot relations<sup>(6)</sup>. Here  $C_0$  is the sound velocity in the medium given by thermodynamics. At high

temperatures,  $T \gg \mu$ , we find  $C_0 = 0.557$ , while at the lowest temperatures under consideration,  $C_0 = 0.538$ . The colliding matter continues to be compressed, with velocity  $W = (1 - 1/\Gamma^2)^{\frac{1}{2}} \approx 1$ . At time  $t_1 = \Delta/(C_0^2 + 1)$ , the shocks reach the outer edges of the disks and matter begins to flow outward from the compacted region of the collision. The region between the outgoing matter front of the shocks and the ingoing matter of the nucleons is the so-called region of the progressive wave solution<sup>(7)</sup>, and although it accounts for only one or two pions, these can carry off up to half the available energy. At the time  $t_1$ <sup>(8)</sup> rarefaction waves start to travel back from the outer edges with velocity  $C_0$ . They meet at the

center at  $t_2 = \frac{1}{C_0}(1 + \frac{1}{C_0}) \frac{\Delta}{2} \frac{C_0^2}{C_0^2 + 1}$ . The entire system at this

instant is described by the progressive wave solution. The temperature is still given by  $T \approx 2E_p^c$ . The system now expands rapidly, pushing the progressive wave regions outward with velocity  $\approx 1$ .

This is the region of the "nontrivial" solution to the hydrodynamic equations<sup>(8)</sup>. The expansion, which is largely one dimensional,

continues until the temperature approaches  $T_c \approx \mu$ . Then the complicated three dimensional phase begins (which can be treated only crudely, but which governs only the minor transverse phenomena).

At  $T_c = \mu$  the whole system disintegrates into particles. The probability of production of a particular species "x" is given

(at least for bosons) by  $\exp(-M_x/T_c)$ , so if  $M_x \gg \mu$ , the "x"

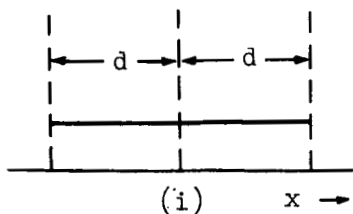
particle species does not occur in significant numbers. Consequently, mainly  $\pi$ 's and a few K's are produced. The number of particles produced is proportional to the total change in entropy as the temperature drops from  $T_0$  to  $T_c$ . The total number of pions produced  $v_\pi$ , or pion multiplicity, is found to be

$$(1) \quad v_\pi = K_\pi [E_p/M]^{1/4}$$

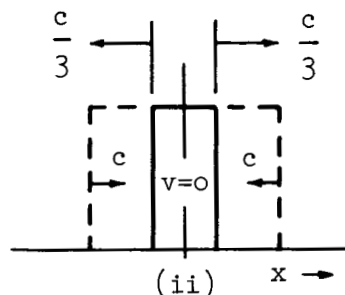
where  $K_\pi$  is given by experimental fit to be of the order of 3.3. Agreement is good for  $E_p$  from about 50 GeV to  $10^4$  GeV. Above  $E_p = 10^4$  GeV, data are scarce but there is some evidence that  $v_\pi$  may be rising more slowly.

### 3. Pion energy and angular distribution in CMS

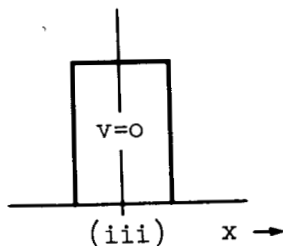
An experimental result<sup>(9)</sup>, of which frequent use is made, is that the average transverse momentum  $\langle P_\perp \rangle$  of the pions is relatively independent of production angle and  $E_p$ . Recall that  $P_\perp$  is a Lorentz invariant  $P_\perp = P_\perp^c$ . The average value of  $P_\perp$  is measured to be 0.4 - 0.7 GeV/c. When we completely ignore the three dimensional expansion stage in the Landau model, we get the most probable value of  $P_\perp$  to be 1-2  $\mu$  as a result of thermal motion. This is of the right order. For the overwhelming majority of pions,  $P_\perp > \mu$ . This is illustrated in Fig. 2, which shows the differential transverse momentum spectra of pions for various incident proton energies (the parameter  $\xi$  reflects the incident proton



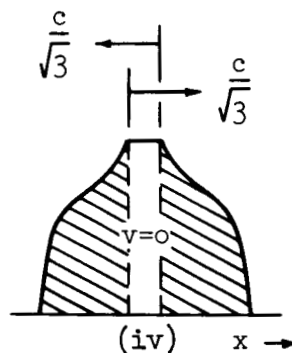
(i) The instant of collision ( $t=t_0$ )



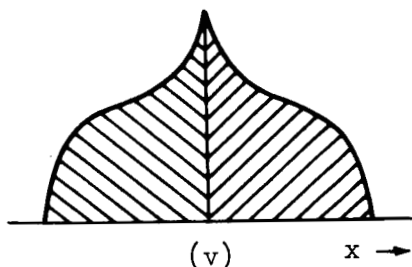
(ii) Shock wave propagates in both directions with velocity  $\frac{c}{3}$ . The matter between shock continues to be compressed with velocity  $c$ ;  $v$ , the velocity of the fluid, is zero between the shocks



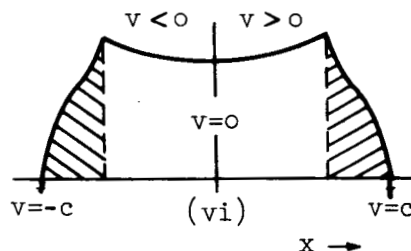
(iii) The shocks have just passed over the matter ( $t=t_1$ )



(iv) The outflow of matter has begun and its effect (the rarefaction wave) is propagating to the center with sound velocity. The flowing region is represented by the progressive solution (shaded area)



(v) The two progressive (rarefaction) waves have just met



(vi) The region of nontrivial solution bounded by the two progressive waves is formed, and expands quickly, pushing the progressive waves into the narrow space very near the wave fronts

Fig. 1 Nucleon-Nucleon Scattering According to the Landau Model  
(Adaption of a Figure from AMAI et al.(5))

Research Dept.  
RE-215J  
June 1965

energy through the dependence  $\sinh(\xi \alpha E_p^{1/2})$ . The distribution curve is peaked near  $P_{\perp}/\mu = 1$  (depending on  $E_p$ ) with a long tail toward higher  $P_{\perp}$ .

In the derivation of the energy and angle distribution of the pion in the center of mass of the colliding protons, we follow MILEKHIN<sup>(10)</sup> in defining the parameters  $\eta$  and  $\zeta$  by:

$$(2) \quad E_{\pi}^c = \mu \cosh \eta \cosh \zeta$$

$$(3) \quad P_{\perp} = \mu \sinh \zeta .$$

Then the CMS emission angle of the pions is given by

$$(4) \quad \tan \theta^c = \tanh \zeta \operatorname{csch} \eta .$$

Milekhin shows that the distribution function

$$(5) \quad \frac{1}{N_{\pi}} \frac{dN_{\pi}}{d\eta} \equiv f(\eta)$$

may be approximated to better than 10 per cent accuracy by a Gaussian

$$(6) \quad f(\eta) \approx \frac{1}{(2\pi L)^{1/2}} \exp(-\eta^2/2L) ,$$

the normalization being

$$(7) \quad \int_{-\infty}^{\infty} f(\eta) d\eta = 1 .$$

The "Landau parameter",  $L$ , is chosen by Milekhin to be

$$(8) \quad L = 0.56 \ln \frac{E_p}{M} + 1.6$$

for nucleon-nucleon collisions; this is slightly higher than the conventional value in order to get a better fit to the angular distribution.

To derive "exact" energy and angle distributions  $f(\eta, \zeta)$ , the distribution in  $\zeta$  for fixed  $\eta$  is also needed. Unfortunately,  $f(\eta, \zeta)$  is not in closed form; however, the energy-angle distributions can be calculated still by employing the result  $P_{\perp} > \mu$  for the vast majority of particles. Consequently in Eq. (3), we set  $\sinh \zeta > 1$ . Immediately, then

$$(9) \quad \tan \theta^c \approx \frac{1}{\sinh \eta},$$

which via the identity:

$$\operatorname{csch}^{-1} x = \ln \left[ x^{-1} + (1 + x^{-2})^{\frac{1}{2}} \right],$$

yields

$$\eta = - \ln \tan \frac{\theta^c}{2},$$

and

$$\left| \frac{d\eta}{d\theta^c} \right| = \frac{1}{2 \tan \frac{\theta^c}{2}} \sec^2 \frac{\theta^c}{2} = \frac{1}{\sin \theta^c}.$$

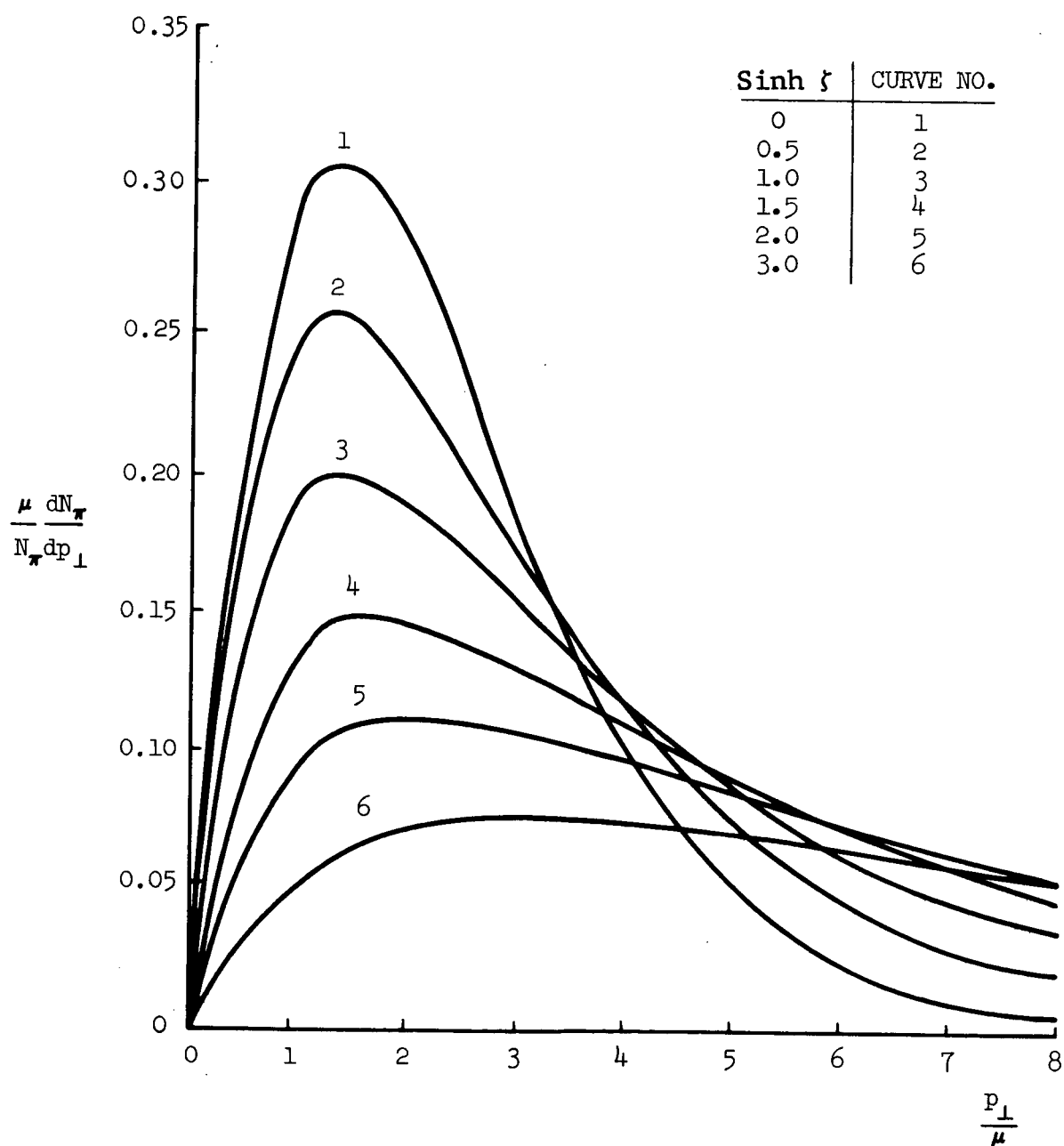


Fig. 2 Pion Transverse Momentum Distribution, After MILEKHIN<sup>(10)</sup>

Thus, the CMS angular distribution is given by

$$\begin{aligned}
 f(\theta^c) &= \frac{1}{N_\pi} \frac{dN_\pi}{d\theta^c} = \frac{f(\eta(\theta^c))}{\sin \theta^c} \\
 (10) \quad &= \frac{1}{(2\pi L)^{\frac{1}{2}}} \cdot \frac{\exp\left[-\frac{1}{2L} \ln^2\left(\tan \frac{\theta^c}{2}\right)\right]}{\sin \theta^c};
 \end{aligned}$$

$f(\theta^c)$  is normalized by

$$\int_0^\pi f(\theta^c) d\theta^c = 1.$$

The form of the function  $f(\theta^c)$  is shown in Fig. 3.

The CMS energy can be expressed as a simple function of the CMS angle through the use of Eqs. (2), (3), and (9), so that

$$(11) \quad E_{\pi^c} \approx \frac{[P_\perp^2 + \mu^2]^{\frac{1}{2}}}{\sin \theta^c}.$$

Because the transverse momenta of all the pions are of the same order of magnitude, their CMS energy may be approximated by either the expression

$$(12a) \quad E_{\pi^c} \approx \frac{[\langle P_\perp^2 \rangle + \mu^2]^{\frac{1}{2}}}{\sin \theta^c}$$



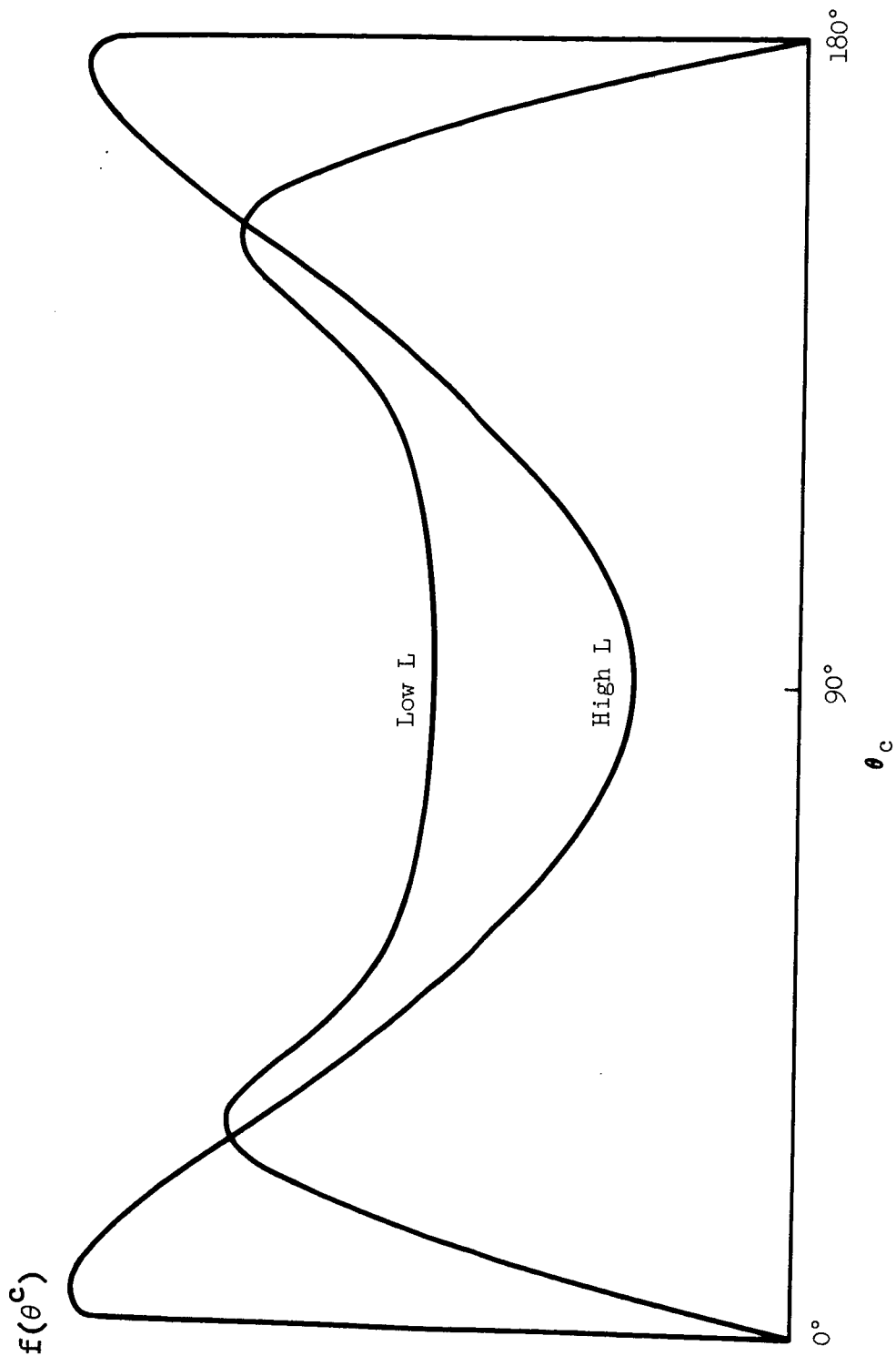


Fig. 3  $f(\theta^c)$ , the Center of Momentum Angular Distribution of Pions, Given by Eq. (10) in Terms of the Center of Momentum Angle  $\theta_c$ .

or, by introducing a constant,  $K$ , which can be determined phenomenologically, may be written\* for all proton energies as

$$(12b) \quad E_{\pi}^c \approx \frac{K}{\sin \theta^c}.$$

One finds  $K \sim 2\mu$ .

Equation (12) allows us to obtain the CMS energy distribution directly from the pions' CMS angular distribution using

$$\frac{d\theta^c}{dE_{\pi}^c} = - \frac{K/E_{\pi}^c}{\left[ (E_{\pi}^c)^2 - K^2 \right]^{\frac{1}{2}}}.$$

We find

$$(13) \quad f(E_{\pi}^c) = \frac{1}{(2\pi L)^{\frac{1}{2}}} \frac{1}{\left[ (E_{\pi}^c)^2 - K^2 \right]^{\frac{1}{2}}} \\ \cdot \exp \left\{ - \frac{1}{2L} \ln^2 \left[ \frac{E_{\pi}^c + \left[ (E_{\pi}^c)^2 - K^2 \right]^{\frac{1}{2}}}{K} \right] \right\}.$$

---

\*The distortion of the basic Landau-Milekhin theory is minimized by replacing the radical in Eq. (11) by a constant. Figure 2 represents  $dN_{\pi}/dP_{\perp}$  as peaked in the neighborhood of  $\mu$  followed by a long tail toward the higher energies. Clearly then, the distribution  $dN_{\pi}/d[P_{\perp}^2]$  will be even more strongly peaked and consequently the replacement of  $P_{\perp}^2$  by  $\langle P_{\perp}^2 \rangle$  is not a severe distortion of the theory's prediction.

As we always consider  $E_{\pi}^c \gg K$ , Eq. (13) may be simplified\* to

$$(14) \quad f(E_{\pi}^c) = \frac{1}{(2\pi L)^{\frac{1}{2}}} \frac{1}{E_{\pi}^c} \exp \left\{ -\frac{1}{2L} \ln^2 \left[ \frac{2E_{\pi}^c}{K} \right] \right\} .$$

Equation (14) seems to reasonably represent the pion distribution from  $E_{\pi}^c \approx K$  to  $E_{\pi}^c \approx \frac{K}{2} e^{(2L)^{\frac{1}{2}}}$  for proton energies  $E_p > 50$  GeV. At pion energies above  $\frac{K}{2} e^{(2L)^{\frac{1}{2}}}$ , the experimental spectrum appears to fall drastically. We can revise these distributions to account for this experimental result by using a distribution of the form given in Eq. (14) for  $E_{\pi}^c$  between  $\mu$  and  $\mu e^{(2L)^{\frac{1}{2}}}$  and set  $f(E_{\pi}^c) = 0$  outside this region. This requires a renormalization of the distribution to satisfy Eq. (7).

---

\*Equation (14) may be alternatively derived by considering

$$E_{\pi}^c \approx K \cosh \eta ;$$

for  $E_{\pi}^c \gg K$  we have  $\eta \gg 1$ ,  $\cosh \eta \approx \frac{1}{2}e^{\eta}$ , and

$$\ln \left[ \frac{2E_{\pi}^c}{K} \right] \approx \eta .$$

The rederivation of Eq. (14) follows then by use of Eq. (6).

Using the "error" integral

$$(15) \quad \Phi(x) \equiv \frac{2}{\sqrt{\pi}} \int_0^x e^{-t^2} dt ,$$

$$(16) \quad f(E_{\pi}^c) = \frac{1}{\Phi(1)} (2/\pi L)^{\frac{1}{2}} \frac{1}{E_{\pi}^c} e^{-\frac{1}{2L} \ln^2 \left[ \frac{E_{\pi}^c}{\mu} \right]}$$

for  $\mu \leq E_{\pi}^c \leq \mu e^{(2L)^{\frac{1}{2}}}$ , zero otherwise (see Fig. 4).

An additional reason for truncating the pion energy distribution is found by analyzing the mean energy  $\langle E_{\pi}^c \rangle$ , as a function of  $L(E_p)$ . If one used Eq. (14) without a cut-off to evaluate  $\langle E_{\pi}^c \rangle$ , one finds

$$(17) \quad \begin{aligned} \langle E_{\pi}^c \rangle &= \int_{\mu}^{\infty} E_{\pi}^c \cdot f(E_{\pi}^c) \cdot dE_{\pi}^c \\ &= \frac{\mu}{2} \cdot \left[ \Phi \left( (L/2)^{\frac{1}{2}} \right) + 1 \right] e^{L/2} \end{aligned}$$

Since for large  $L$ ,  $\Phi((L/2)^{\frac{1}{2}}) \approx 1$ ,  $\langle E_{\pi}^c \rangle$  will increase as  $e^{L/2}$ . This is not physical — a glance at Eq. (14) shows that most particles will have  $E_{\pi}^c < e^{(2L)^{\frac{1}{2}}}$ . However, with the cut off we find

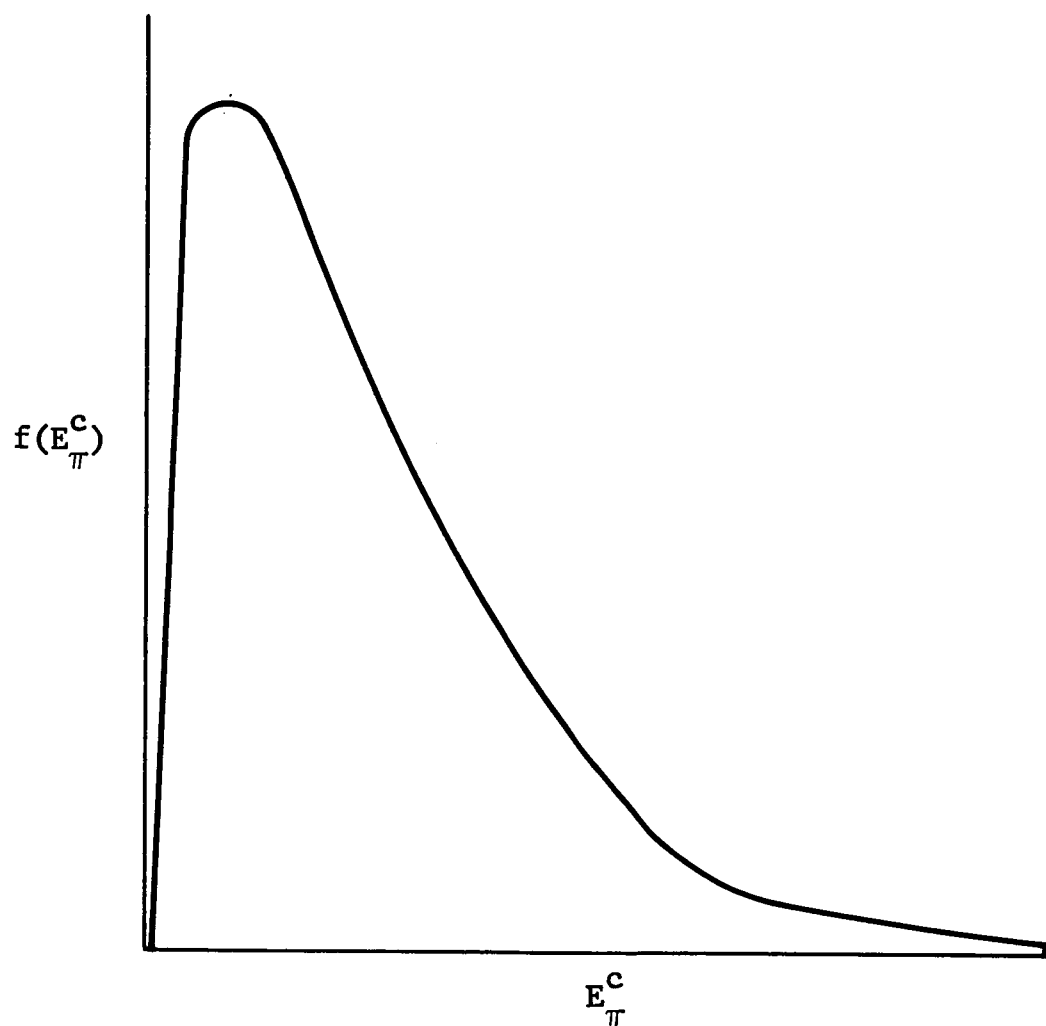


Fig. 4  $f(E_{\pi}^c)$ , Center of Mass Energy Distribution of Pions,  
Given by Eq. (16).

$$\langle E_{\pi}^c \rangle = \int_{\mu}^{\mu} e^{(2L)^{\frac{1}{2}}} E_{\pi}^c f(E_{\pi}^c) dE_{\pi}^c$$

(18)

$$= \frac{\mu}{\Phi(1)} e^{L/2} \left[ \Phi \left[ (L/2)^{\frac{1}{2}} \right] - \Phi \left[ (L/2)^{\frac{1}{2}} - 1 \right] \right] .$$

Here, for large energies,

$$\Phi \left[ (L/2)^{\frac{1}{2}} \right] - \Phi \left[ (L/2)^{\frac{1}{2}} - 1 \right] \approx \Phi' \left[ (L/2)^{\frac{1}{2}} \right] = \frac{2}{\sqrt{\pi}} e^{-L/2} ,$$

which, using the asymptotic formula

$$\Phi(z) \approx 1 - \frac{2}{\sqrt{\pi}} \frac{e^{-z^2}}{2z} \left\{ 1 - \frac{1}{2z^2} \right\} ,$$

leads to

$$\frac{\langle E_{\pi}^c \rangle}{\mu e^{(2L)^{\frac{1}{2}}}} \approx \frac{e^{-1}}{\Phi(1) \sqrt{\pi}} \left[ \frac{1}{(L/2)^{\frac{1}{2}} - 1} \right] ,$$

which decreases as  $L$  increases and is always less than 1, satisfying the physical requirements.

The cut-off in CMS energy implies a cut-off in the angular distribution near  $\theta^c = 0, \pi$ . A renormalization in the calculation similar to that involved in Eq. (16) gives the angular distribution

$$(19) \quad f(\theta^c) = \frac{1}{\Phi(1) (2\pi L)^{\frac{1}{2}}} \frac{\exp\left\{-\frac{1}{2L} \ln^2 \tan \frac{\theta^c}{2}\right\}}{\sin \theta^c}$$

for  $\theta_{\min}^c < \theta^c < \theta_{\max}^c$ , where

$$\frac{\theta_{\min}^c}{2} = \tan^{-1} e^{-(2L)^{\frac{1}{2}}},$$

$$\frac{\theta_{\max}^c}{2} = \tan^{-1} e^{(2L)^{\frac{1}{2}}} = \frac{\pi}{2} - \frac{\theta_{\min}^c}{2}.$$

The integral energy distribution defined through

$$G(E_{\pi}^c) \equiv \int_{\mu}^{E_{\pi}^c} f(E_{\pi}^c) dE_{\pi}^c$$

is found to be

$$G(E_{\pi}^c) = \frac{1}{\Phi(1)} \Phi \left[ \frac{1}{(2L)^{\frac{1}{2}}} \ln \frac{E_{\pi}^c}{\mu} \right]$$

$$(20) \quad \begin{aligned} &= 0 \quad \text{if} \quad E_{\pi}^c < \mu \\ &= 1 \quad \text{if} \quad E_{\pi}^c > \mu e^{(2L)^{\frac{1}{2}}}. \end{aligned}$$

In Table 1 we have tabulated  $G(E_{\pi}^c)$ . Columns 1 and 2 correspond to incident proton energies of  $10^2$  and  $10^8$  GeV respectively; Column 3 is introduced to permit the use of the table for calculations of arbitrary incident proton energies.

TABLE 1

INTEGRAL ENERGY DISTRIBUTION:  $G(E_{\pi}^c)$

$E_{\pi}^c / \mu_{\pi}$	$E_{\pi}^c / \mu_{\pi}$	$\frac{1}{(2L)^{\frac{1}{2}}} \ln \frac{E_{\pi}^c}{\mu_{\pi}}$	$G(E_{\pi}^c)$
$(E_p = 10^2 \text{ GeV})$	$(E_p = 10^8 \text{ GeV})$		
1.24	1.44	.075	.10
1.54	2.08	.15	.20
1.73	2.53	.19	.25
3.00	6.69	.395	.50
6.05	22.20	.638	.75
7.39	29.96	.695	.80
11.02	54.60	.828	.90
13.46	81.45	.910	.95

Similarly, the integral angular distribution  $G(\theta^c)$ , the fraction of particles with  $\theta < \theta_c$  is found via Eq. (19) to be given by

$$\begin{aligned}
 G(\theta^c) &= \frac{1}{2} + \frac{1}{2\Phi(1)} \Phi \left[ \frac{1}{(2L)^{\frac{1}{2}}} \ln \left( \tan \frac{\theta^c}{2} \right) \right] \\
 (21) \quad &= 0 \quad \text{if} \quad \theta < \theta_{\min}^c \\
 &= 1 \quad \text{if} \quad \theta > \theta_{\max}^c .
 \end{aligned}$$

This function is tabulated in Table 2.



TABLE 2  
INTEGRAL ANGULAR DISTRIBUTION:  $G(\theta^c)$

$\theta^c$ $E_p = 10^2 \text{ GeV}$	$\theta^c$ $E_p = 10^8 \text{ GeV}$	$\frac{1}{(2L)^{\frac{1}{2}}} \ln \tan \frac{\theta^c}{2}$	$G(\theta^c)$
39°	17°	-0.39	0.25
90°	90°	0	0.50
114°	129°	0.15	0.60
152°	167°	0.485	0.80
164°	177°	0.695	0.90
169°	178°	0.830	0.95

#### 4. Distribution of pions in the laboratory frame

A form for the energy distribution of the pions, which will be independent of the angle of production, can be arrived at through a relationship between the pion laboratory energy,  $E_\pi$ , and the hydrodynamic variable " $\eta$ " [see Eq. (6)]. To obtain this relation let us consider the expression for the laboratory pion energy

$$(22) \quad E_\pi = E_\pi^c \Gamma(1 + \beta_\pi^c \cdot \cos \theta^c) .$$

This can be replaced for high energy pions by the Doppler form

$$(23) \quad E_\pi = E_\pi^c \Gamma(1 + \cos \theta^c)$$

(for  $E_p = 10^2 \text{ GeV}$ ,  $\langle \beta_\pi^c \rangle = .98$ ). The angular function in Eq. (23) can be replaced after some manipulation of Eq. (14) by

$$\cos \theta^c = \frac{\sinh \eta}{(\sinh^2 \eta + \tanh^2 \zeta)^{\frac{1}{2}}} .$$

When  $\cos \theta^c$  is placed in Eq. (23) we find, after employing the usual Landau approximation  $\tanh \zeta = 1$ , that

$$(24) \quad E_{\pi} = \mu \Gamma \cosh \eta \cosh \zeta [1 + \tanh \eta] .$$

We can remove the last of the " $\zeta$ " dependence by utilizing the constancy of the transverse momentum [see Eqs. (3) and (12)] so that

$$(25) \quad E_{\pi} = K \Gamma \cosh \eta [1 + \tanh \eta]$$

$$E_{\pi} = K \Gamma e^{\eta} .$$

Because

$$f(E_{\pi}) = \frac{1}{N_{\pi}} \frac{dN_{\pi}}{dE_{\pi}} = \frac{1}{N_{\pi}} \frac{dN_{\pi}}{d\eta} \left| \frac{d\eta}{dE_{\pi}} \right| ,$$

it follows immediately from Eqs. (6) and (25) that

$$(26) \quad f(E_{\pi}) = \frac{1}{E_{\pi} [2\pi L]^{\frac{1}{2}}} \exp \left\{ \frac{-1}{2L} \ln^2 \frac{E_{\pi}}{K\Gamma} \right\} .$$

Equation (26), like Eq. (6), is normalized upon the assumption of an infinite upper limit for the pion energies. To normalize the laboratory frame distribution as had been done for the c.m., we need to determine the energy limits in the laboratory frame. These can be obtained by considering the use of Eq. (12) in Eq. (23):

$$(27) \quad E_{\pi} = E_{\pi}^c \Gamma \left[ 1 \pm \left\{ 1 - \left[ \frac{K}{E_{\pi}^c} \right]^2 \right\}^{\frac{1}{2}} \right],$$

the ambiguity sign referring to either motion "forward",  $\cos \theta^c > 0$ , or "backward",  $\cos \theta^c < 0$ , in the CMS. Then  $E_{\pi}^c \gg K$  reduces Eq. (25) to

$$(28) \quad \begin{aligned} E_{\pi} &= 2\Gamma E_{\pi}^c && \text{("forward" in CMS)} \\ E_{\pi} &= \frac{2\mu^2 \Gamma}{E_{\pi}^c} && \text{("backward" in CMS).} \end{aligned}$$

Consequently, the energy limits for the laboratory distribution are

$$(29a) \quad E_{\pi} \Big|_{\max} = 2\mu\Gamma \exp(2L)^{\frac{1}{2}}$$

$$(29b) \quad E_{\pi} \Big|_{\min} = 2\mu\Gamma \exp(-2L)^{\frac{1}{2}}.$$

Renormalizing Eq. (26) with these limits gives

$$(30) \quad f(E_{\pi}) = \frac{A_{\pi}}{E_{\pi}} \exp \left( \frac{-1}{2L} \ln^2 \frac{E_{\pi}}{K\Gamma} \right),$$

where

$$A_{\pi} \approx \left[ \Phi(1) (2\pi L)^{\frac{1}{2}} \right]^{-1}.$$

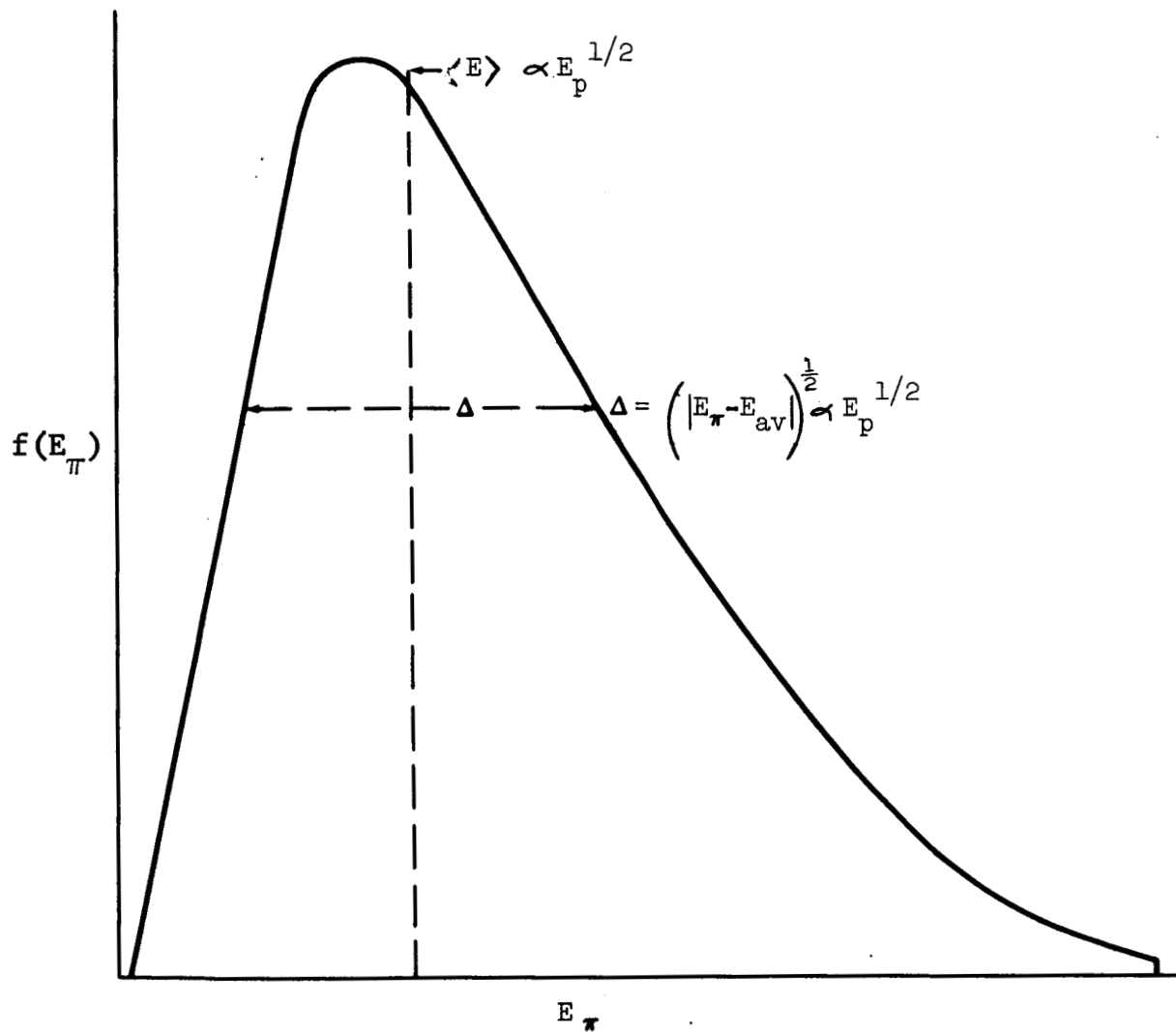


Fig. 5 Laboratory Energy Distribution of Pions,  
 $f(E_\pi)$  from Eq. (30).

Equation (30) then gives the omnidirectional energy distribution function for pions produced by a proton of energy  $E_p$ ; this function is illustrated in Fig. 5. In Section 5 we utilize this distribution to calculate the pion energy distribution in space due to cosmic ray collisions.

The angular distribution of the pions can be readily found through the relativistic angular transformation

$$(31) \quad \tan \theta = \frac{1}{\Gamma} \cdot \frac{\sin \theta^c}{\cos \theta^c + \frac{W}{\beta_{\pi} c}} .$$

As in the energy distribution for high energy pions, Eq. (31) may be written in a Doppler form

$$\tan \theta = \frac{1}{\Gamma} \tan[\theta^c/2] .$$

Incorporating Eq. (19) and (31) into the distribution formula

$$f(\theta) = \frac{1}{N_{\pi}} \frac{dN_{\pi}}{d\theta} = f(\theta^c\{\theta\}) \cdot \left| \frac{d\theta^c}{d\theta} \right| ,$$

we get for  $\theta_{\min} < \theta < \theta_{\max} < \pi/2$ ,

$$(32) \quad f(\theta) = \frac{2A}{\sin 2\theta} \exp \left[ \frac{-1}{2L} \ln^2 \left\{ \Gamma \tan \theta \right\} \right] ,$$

and for  $\theta > \theta_{\max}$  or  $\theta < \theta_{\min}$ ,

$$f(\theta) = 0 .$$

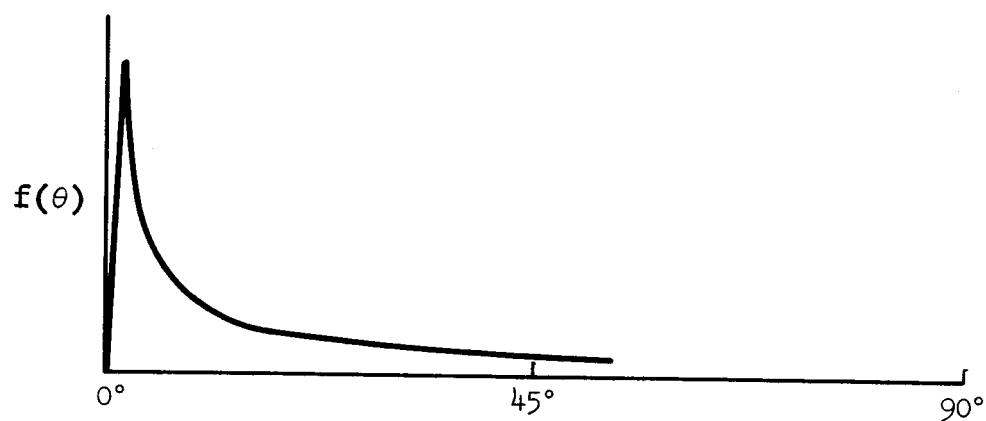


Fig. 6 Laboratory Angular Distribution of Pions  
Produced in a Single Collision

The range of  $f(\theta)$  is established from Eqs. (19) and (31) to be

$$\theta_{\min} = \tan^{-1} \left[ \frac{\exp\{-2L\}^{\frac{1}{2}}}{\Gamma} \right]$$

(33)

$$\theta_{\max} = \tan^{-1} \left[ \frac{\exp\{2L\}^{\frac{1}{2}}}{\Gamma} \right] .$$

Equation (32) indicates an angular distribution in the laboratory that is peaked strongly in the forward direction. The peak will be to the left of  $\theta = \tan^{-1}(1/\Gamma)$  in the distribution. For 50 GeV cosmic rays, where  $\tan^{-1}(1/\Gamma) = 14.8$  degrees, the distribution peaks in the forward direction at  $\theta < 0.6$  degrees (see Fig. 6).

A useful quantity often referred to in the literature is the angle in the laboratory corresponding to  $\theta^c = 90^\circ$ , within which angle [Table 2, or by the obvious symmetry in  $f(\theta^c)$ ] half the pions are contained. This angle is often denoted  $\theta_{\frac{1}{2}} = \tan^{-1}(1/\Gamma)$ . Experimentally  $\theta_{\frac{1}{2}}$  gives a measure of the incident cosmic ray energy  $E_p$  via  $\Gamma = \left( \frac{\gamma_p + 1}{2} \right)^{\frac{1}{2}}$  that is,

$$E_p = M(2 \tan^2 \theta_{\frac{1}{2}} - 1) .$$

One must be cautious about using this equation in the general literature, as experimental situations usually deal with nucleon-nucleus collisions<sup>(11,12)</sup> where the assumption of CMS symmetry about  $\theta_c = 90^\circ$  is rather dubious.

The particle number is a Lorentz invariant. Therefore we may find  $G(\theta)$ , the integral distribution function in the laboratory frame, merely by transforming angles

$$G(\theta) = \frac{1}{2} + \frac{1}{2\Phi(1)} \Phi \left[ \frac{1}{(2L)^{\frac{1}{2}}} \ln(\Gamma \tan \theta) \right].$$

The table of values, Table 2, is then valid in the laboratory frame if the last two column headings are changed to  $1/(2L)^{\frac{1}{2}} \times \ln(\Gamma \tan \theta)$  and  $G(\theta)$ , respectively, and if the CMS angle columns are ignored.

Tables 3 and 4 give the results of calculations using the above formulas, with incident energies ranging from  $E_p \sim 10^2$  GeV to  $10^{11}$  GeV, including cut-offs, "means," and 80 per cent values of the integral spectra.

## 5. The cosmic ray pion source function

A useful extension of the pion energy distribution [see Eq. (30)] is the cosmic ray pion source distribution, the number of pions produced in the energy range  $E_\pi$  to  $E_\pi + dE_\pi$  by cosmic ray protons colliding with matter space of density  $n$  protons  $\text{cm}^{-3}$  and cross section  $\sigma_{pp}$ . The pion source function can be written as

$$(34) \quad q_\pi(E_\pi) dE_\pi = n \sigma_{pp} \int j_p(E_p) \cdot v_\pi(E_p) \cdot f_\pi(E_\pi, E_p) \cdot dE_p \cdot dE_\pi$$

where  $j_p(E_p)$  is the cosmic ray flux, which can be represented by the power law  $K_p E_p^{-\eta} \text{ cm}^{-2} \text{ sr}^{-1} \text{ GeV}^{-1} \text{ sec}^{-1}$  ( $\eta \approx 2.6$ ), and the



TABLE 3

ENERGY DISTRIBUTION CALCULATIONS

Incident Energy $\gamma_p$	Landau Parameter L	Expected $\pi$ Multiplicity $N_\pi$	Lab Transf'n of CMS $\Gamma$	CMS Energies ( $\pi$ 's) Max $\gamma_\pi^c$	Mean $\gamma_\pi^c$	80% Limit $\gamma_\pi^c$
$10^2$	4.18	5.3	7.14	18.0	4.64	7.46
$10^3$	5.47	9.5	$2.24 \times 10^1$	27.4	6.11	9.97
$10^4$	6.76	16.5	$7.07 \times 10^1$	39.6	8.02	12.8
$10^5$	8.05	30.0	$2.24 \times 10^2$	55.1	9.90	16.1
$10^6$	9.34	53.0	$7.07 \times 10^2$	75.2	12.5	20.1
$10^7$	10.63	95.0	$2.24 \times 10^3$	100.5	15.2	24.5
$10^8$	11.92	168.0	$7.07 \times 10^3$	131.6	18.9	29.7
$10^9$	13.21	299.0	$2.24 \times 10^4$	170.0	22.1	35.5
$10^{10}$	14.50	532.0	$7.07 \times 10^4$	220.0	27.9	42.1
$10^{11}$	15.79	946.0	$2.24 \times 10^5$	273.0	33.4	49.4

Ref. Formulas (8)

(1)

(16)

(17)

Table 1

TABLE 4

## ANGULAR DISTRIBUTION CALCULATION

Incident Energy $\gamma_p$	Landau Parameter L	Lab Transf'n of CMS $\Gamma$	CMS Extrema Angle ( $\theta_{\max}^c = \pi - \theta_{\min}^c$ )		Lab Angles		
			(Radians)	(Degrees)	$\theta_{\min}$ (Radians)	50% Angle Limit (Radians)	80% Angle Limit (Radians) $\theta_{\max}$
$10^2$	4.18	7.14	$1.12 \times 10^{-2}$	6° 22'	$7.80 \times 10^{-3}$	$1.40 \times 10^{-1}$	$5.17 \times 10^{-1}$ 1.19
$10^3$	5.47	$2.24 \times 10^1$	$7.30 \times 10^{-2}$	4° 10'	$1.63 \times 10^{-3}$	$4.50 \times 10^{-2}$	$2.18 \times 10^{-1}$ $8.86 \times 10^{-1}$
$10^4$	6.76	$7.07 \times 10^1$	$5.1 \times 10^{-2}$	2° 56'	$3.61 \times 10^{-4}$	$1.41 \times 10^{-2}$	$8.35 \times 10^{-2}$ $5.06 \times 10^{-1}$
$10^5$	8.05	$2.24 \times 10^2$	$3.62 \times 10^{-2}$	2° 26'	$8.08 \times 10^{-5}$	$4.47 \times 10^{-3}$	$3.14 \times 10^{-2}$ $2.42 \times 10^{-1}$
$10^6$	9.34	$7.07 \times 10^2$	$2.66 \times 10^{-2}$	1° 32'	$1.86 \times 10^{-5}$	$1.41 \times 10^{-3}$	$1.14 \times 10^{-2}$ $1.06 \times 10^{-1}$
$10^7$	10.63	$2.24 \times 10^3$	$1.9 \times 10^{-2}$	1° 8'	$4.44 \times 10^{-6}$	$4.47 \times 10^{-4}$	$4.22 \times 10^{-3}$ $4.50 \times 10^{-2}$
$10^8$	11.92	$7.07 \times 10^3$	$1.52 \times 10^{-2}$	52'	$1.07 \times 10^{-6}$	$1.41 \times 10^{-4}$	$1.52 \times 10^{-3}$ $1.86 \times 10^{-2}$
$10^9$	13.21	$2.24 \times 10^4$	$1.16 \times 10^{-2}$	40'	$2.59 \times 10^{-7}$	$4.47 \times 10^{-5}$	$5.40 \times 10^{-4}$ $7.21 \times 10^{-3}$
$10^{10}$	14.80	$7.07 \times 10^4$	$9.0 \times 10^{-3}$	31'	$6.36 \times 10^{-8}$	$1.41 \times 10^{-5}$	$1.92 \times 10^{-4}$ $3.14 \times 10^{-3}$
$10^{11}$	15.79	$2.24 \times 10^5$	$7.2 \times 10^{-3}$	25'	$1.61 \times 10^{-8}$	$4.47 \times 10^{-6}$	$6.88 \times 10^{-5}$ $1.23 \times 10^{-3}$

Ref. Formulas (8)

(19b)

(33)

Table 2

(33)

factor  $v_{\pi} f_{\pi} dE_{\pi}$  is the number of pions with energy between  $E_{\pi}$  and  $E_{\pi} + dE_{\pi}$  produced in a collision by a proton with energy  $E_p$ . The thermal energy of the target nucleon is negligible when compared to the incident cosmic ray proton.

Equation (34) can be written explicitly using Eqs. (1) and (30) as

$$q_{\pi}(E_{\pi}) dE_{\pi} = K_p K_{\pi} \frac{n\sigma_{pp}}{E_{\pi}} \int_{E_{p1}}^{E_{p2}} A_{\pi} E_p^{-\eta + \frac{1}{4}} \cdot \exp\left\{\frac{-1}{2L} \ln^2 \left[ \frac{E_{\pi}}{2\mu\Gamma} \right]\right\} dE_p dE_{\pi} \quad (35)$$

pions/cm<sup>3</sup> sr GeV sec.

The limits of integration are arrived at by inverting Eqs. (29). This integral is evaluated in the Appendix where it is found to be

$$q_{\pi}(E_{\pi}) dE_{\pi} = \frac{K_p K_{\pi} n\sigma_{pp}}{2\mu\Phi(1)k} \exp(3.2\eta - 2.4) \cdot \left\{ e^{-2kv} \left[ \Phi\left(\frac{v}{u_1} - ku_1\right) + \Phi\left(\frac{v}{u_2} - ku_2\right) \right] - e^{2kv} \left[ \Phi\left(\frac{v}{u_1} + ku_1\right) - \Phi\left(\frac{v}{u_2} + ku_2\right) \right] \right\} dE_{\pi} \quad (36)$$

where

$$k = (2\eta - 2)^{\frac{1}{2}}, \quad v = \frac{1}{\sqrt{2}} \ln \frac{E_{\pi} e^{1.6}}{\mu \sqrt{2}},$$

$$u_1 = 2^{-\frac{1}{2}} \left[ -1 + \left\{ 1 + 2\sqrt{2} z \right\}^{\frac{1}{2}} \right],$$

and

$$u_2 = 2^{-\frac{1}{2}} \left[ 1 + \left\{ 3.78 + 2\sqrt{2} z \right\}^{\frac{1}{2}} \right].$$

Equation (36) has been evaluated and plotted by an electronic computer (IBM 7094). The plotted results are shown as the solid curve in Fig. 7. The results of GINZBURG and SYROVATSKI<sup>(13)</sup> are plotted, for comparison, as the broken line. The figure indicates that Eq. (36) can be well approximated by the power law

$$q_{\pi}(E_{\pi}) dE_{\pi} = C_{\pi} E_{\pi}^{-z} \frac{\text{Pions}}{\text{cm}^3 \text{ sr GeV sec}}$$

where  $z \approx 3.26$ , and  $C_{\pi} = 7.2 n\sigma_{pp}$  when  $\eta = 2.6$ ,  $K_p = 1.5$ , and  $K_{\pi} = 3.3$ .

A recent experimental paper by KIM<sup>(1)</sup> compares Landau model predictions with experimental results in the case of the pion's transverse momentum and angular distribution in the CMS frame. There it is found that agreement is good. It is hoped that the form in which the angular and energy distribution are presented

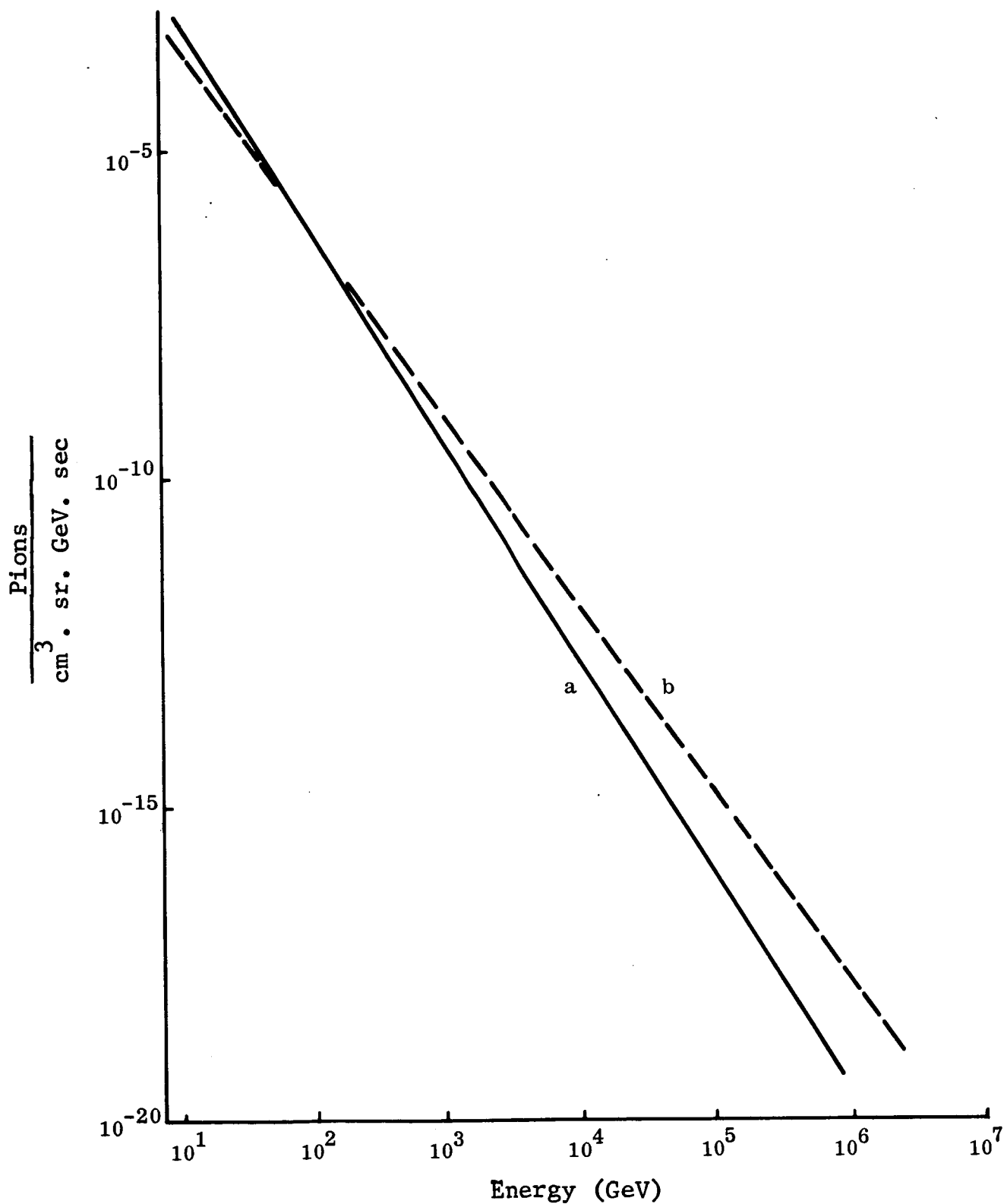


Fig. 7 Pion Source Function in Space ( $n \sigma_{pp} \equiv 1$ ) from Cosmic Ray Collisions: a) Hydrodynamic Model (present paper); b) GINZBURG-SYROVATSKI<sup>(15)</sup>

above are of a nature that will help lead to an improved description of the production of pions. It seems certain that the peripheral model alone will not describe this phenomenon.

Extensions of the pion energy distribution to the calculations of the high energy gamma ray background in space has been carried out by LIEBER, MILFORD, and SPERGEL<sup>(14)</sup>. Further details of the gamma ray calculation and some of the present pion calculation can be found in Ref. 15. SPERGEL and SCANLON<sup>(16)</sup> have calculated an approximate high energy electron production spectrum in space.

## REFERENCES

- (1) C. O. KIM: Phys. Rev., 136, B515 (1964).
- (2) G. FUJIOKA, Y. MAEDA, O. MINAKAWA, M. MIYAGAKI, Y. TSUZUKI, I. MITO, K. KOBAYAKAWA, H. SHIMOIDA, H. NAKATANI, O. KUSUMOTO, K. NIU, and K. NISHIKAWA: Suppl. Nuovo Cimento, Series I, 1, 1143 (1964).
- (3) E. FERMI: Progr. Theoret. Phys. (Kyoto), 5, 570 (1950); Phys. Rev., 81, 683 (1951); 92, 452 (1953); 93, 1436 (1954).
- (4) L. D. LANDAU: Izv Akad Nauk SSSR Ser. Fiz., 17, 51 (1953); G. A. MILEKHIN: Soviet Physics (JETP), 8, 829 (1959); I. L. ROZENTAL and D. S. CHERNAVSKII: Usp. Fiz. Nauk., 52, 185 (1954).
- (5) S. AMAI, H. FUKADA, C. ISO, M. SATO: Progr. Theoret. Phys. (Kyoto), 17, 241 (1957).
- (6) I. M. KHALATNIKOV: Zh. Eksp. Teor. Fiz., 27, 529 (1954).
- (7) N. M. GERASIMOVA and D. S. CHERNAVSKII: Zh. Eksp. Teor. Fiz., 29, 372 (1955).
- (8) S. AMAI et al., Op. Cit.
- (9) W. GALBRAITH: Extensive Air Showers, Academic Press, N.Y. (1958).
- (10) G. A. MILEKHIN, Soviet Physics (JETP), 8, 829 (1959).

- (11) M. F. KAPLON and D. M. RITSON: Phys. Rev., 88, 386 (1952).
- (12) D. H. PERKINS: "Cosmic Rays," Progress in Elementary Particles and Cosmic Ray Physics, Vol. V, Interscience Press, N.Y. (1960).
- (13) V. L. GINZBURG and S. I. SYROVATSKII: The Origin of Cosmic Rays, Pergamon Press, London (1964).
- (14) M. LIEBER, S. N. MILFORD, and M. S. SPERGEL: Annales D'Astrophysique, 28, 202 (1965).
- (15) M. LIEBER, S. N. MILFORD, and M. S. SPERGEL, Grumman Research Department Report RE-192, October 1964.
- (16) M. S. SPERGEL and J. H. SCANLON: Grumman Research Department Report RE-213J also submitted to Nuovo Cimento (1965).



# APPENDIX

We consider below the evaluation of the integral form of the pion source function that appears in Eq. (36) of the text:

$$(A.1) \quad q_{\pi}(E_{\pi}) dE_{\pi} = \frac{K_p K_{\pi} n \sigma_{pp}}{(2\pi)^{\frac{1}{2}} E_{\pi} \Phi(1)} \cdot \int_{E_{p1}}^{E_{p2}} \frac{E_p^{-\eta+\frac{1}{4}}}{L^{\frac{1}{2}}} \exp\left\{\frac{-1}{2L} \ln^2\left(\frac{E_{\pi}}{2\mu\Gamma}\right)\right\} dE_p dE_{\pi}.$$

When we introduce the substitution  $z_{\pi} = \ln \frac{E_{\pi} e^{1.6}}{\sqrt{2} \mu}$  and recall that  $L = \frac{1}{2} \ln \gamma_p + 1.6$ , Eq. (A.1) may be written as

$$(A.2) \quad q_{\pi}(E_{\pi}) dE_{\pi} = C \int_{A_1}^{A_2} \frac{dL}{L^{\frac{1}{2}}} \exp\left[2(\eta - 1)L + z_{\pi}^2/2L\right] dE_{\pi},$$

where

$$C = \frac{K_p K_{\pi} e^{3.2\eta-2.4}}{n \sigma_{pp} \mu \Phi(1) \pi^{\frac{1}{2}}}.$$

When the further substitution  $u = L^{\frac{1}{2}}$  is made, Eq. (A.2) becomes

$$(A.3) \quad q_{\pi}(E_{\pi}) dE_{\pi} = 2C \int_{B_1}^{B_2} du \exp \left[ 2(\eta - 1)u^2 + z_{\pi}^2/2u^2 \right] dE_{\pi}.$$

Integrals of the form of Eq. (A.3) have been evaluated by SPERGEL and SCANLON<sup>(4)</sup>. Using Eq. (B.1) of their paper Eq. (A.3) immediately becomes

$$(A.4) \quad q_{\pi}(E_{\pi}) dE_{\pi} = \frac{C}{2k} \left\{ e^{-2kv} \left[ \Phi \left( \frac{y}{u} - ku \right) \right]_{B_2}^{B_1} + e^{2kv} \left[ \Phi \left( \frac{y}{u} + ku \right) \right]_{B_1}^{B_2} \right\},$$

where  $k = (2\eta - 2)^{\frac{1}{2}}$ ,  $v = (z_{\pi}/2)^{\frac{1}{2}}$ . The determination of the limits for Eq. (A.1) and consequently Eq. (A.4) follows from Eqs. (29) in the text. The minimum proton energy,  $E_{p_1}$ , that can contribute to Eq. (A.1) is the proton energy that satisfies Eq. (29a) for the pion energy in question. The maximum proton energy that can contribute pions follows from Eq. (29b). Equations (29) can

be solved readily for  $L$  or  $u$ . In terms of  $u_1$  and  $u_2$ , Eqs. (29) can be written as

$$(A.3) \quad E_{\pi} = \sqrt{2} \mu e^{u_1^2 + u_1 \sqrt{2} - 1.6}$$

$$(A.4) \quad E_{\pi} = \frac{\mu}{2\sqrt{2}} e^{u_2^2 - u_2 \sqrt{2} - 1.6},$$

and one finds immediately

$$(A.5) \quad u_1 = 2^{-\frac{1}{2}} \left[ -1 + \left( 1 + 2 \ln \frac{E_{\pi} e^{1.6}}{\mu \sqrt{2}} \right)^{\frac{1}{2}} \right]$$

and

$$(A.6) \quad u_2 = 2^{-\frac{1}{2}} \left[ 1 + \left( 1 + 2 \ln \frac{2\sqrt{2} E_{\pi} e^{1.6}}{\mu} \right)^{\frac{1}{2}} \right],$$

as only  $u > 0$  is a physical solution for  $u$ .